



Characterization of myocardium anomalies using watershed-based segmentation approaches in nuclear cardiology

Background: Nuclear cardiology can detect both ischemia and inflammation of the heart. It's difficult to distinguish adjacent tissues in a cardiac scintigraphy image.

Objectives: The aim of the study is to characterize of myocardium anomalies using watershed-based segmentation approaches in nuclear cardiology. The researchers seek to detect heart tissue in nuclear medicine pictures by using watershed methods. The contrast is blurred, and the presence of fleck noise complicates interpretation.

Methods: Thus, color-based image processing can considerably boost the rate of cardiac detection in digital image processing. This study employed color-based k-means clustering. Color space conversion was carried out using scintographs. Following that, using color analysis tools, the image was segmented.

Results: On exhibit was an altogether new and crystal-clear rendition of the segmented scintograph. The proposed method precisely defines the cardiac tissues and their borders. We calculated both the accuracy rate and the recall reckoning. $98.9+9.01$ ($p>0.05$) and $0.07+0.004$ ($p>0.05$) were the results.

Conclusion: The proposed approach is used to identify cardiac tissue precisely.

KEYWORDS: Cardiac tissues • K-means methods • Nuclear medicine

Introduction

Recently, imaging has emerged as a vital tool for surgical planning, disease progression monitoring, and the development of novel therapeutic alternatives. It has since become a widely used standard tool for assisting in the selection of non-invasive therapy. In some instances, nuclear cardiology may be able to aid in the detection and evaluation of coronary artery disease. It is useful for diagnosing cardiomyopathy and other heart-related problems, as well as heart damage caused by a variety of illnesses and injuries [1-3]. It is possible to integrate multiple medical imaging tools using computational and image processing techniques, and the differences between scintographs acquired from different vantage points, at different acquisition times, or even with a subject atlas to obtain prior anatomical or functional information, are more easily recognized and analyzed [4-6]. By highlighting changes in size, shape, or image intensity over time, as well as by comparing preoperative imaging and surgical plans to the actual anatomy observed during surgery, it is feasible to compare patient anatomy to that of a standardized atlas [7-9]. Due to the SPECT imaging protocol's inability to utilize computational tools, a variety of concerns arise that can be utilized to compare

the protocol's performance to the subjective diagnostic technique. Using segmentation, users can simplify or modify the representation of an image into different areas of interest by dividing it into multiple pixel sets called segments. Using the solution to the problem as a starting point, we can determine the level of subdivision needed. Using labels assigned to each pixel in an image, it divides the image into the areas, objects, and contours that make up the image [10-12]. Within a segmented region, each area has properties that are similar to pixels but are significantly different from the next area in terms of certain calculated properties. Most image segmentation algorithms work by separating images into groups based on intensity or region. Make use of the first approach to partition an image based on abrupt intensity changes, such as border lines, in order to create a new image [13]. A number of predefined criteria must be met in order for areas to qualify as regions under the second approach. Biotechnology, video surveillance, traffic management, biology, and microscopy are just a few of the industries that use image segmentation to make their products more efficient [3,5-7]. For disease and tumor diagnosis, as well as for tissue volume measurement, diagnostics, as well as for the study of anatomy and surgery, it is a critical

Yousif Abdallah^{1,2,3*},
Galaleldin Ibrahim⁴,
Nouf Abuhadi⁵, Ghazali
M. Abdel Gadir^{6,7} &
Elabbas Ebaid⁸

¹Department of Radiological Science and Medical Imaging, College of Applied Medical Sciences, Majmaah University, 11952, Majmaah, Saudi Arabia

²College of Radiological Studies and Nuclear Medicine, National Rabit University, Khartoum, Sudan

³Sudan University of Science and Technology, College of Medical Radiological Science, Elbaladi Street, 1908, Khartoum, Sudan

⁴Armed Forces Hospital of Southern Region, Prince Khalid Bin Sultan Cardiac Center, Saudi Arabia

⁵Diagnostic Radiographic Technology Department, College of Applied Medical Science, Jazan University, Jazan, Saudi Arabia

⁶Department of Internal Medicine, College of Medicine, Majmaah University, Al-Majmaah 11952, Saudi Arabia

⁷Department of Medicine, Faculty of Medicine and Health Sciences, Omdurman Islamic University, Sudan

⁸Department of Radiology, College of Medicine, Majmaah University, Al-Majmaah 11952, Saudi Arabia

*Author for correspondence
y.yousif@mu.edu.sa

diagnostic tool. When SPECT images of the myocardial infusion were used, the experimental implementation of the Otsu method, k-means clustering, regional growth, and shape detection were evaluated for comparison. The methods described in the following sections are in-depth. The use of a threshold value allows researcher to distinguish between objects and the background in the image [5,8]. As soon as the threshold is set to T , the object point is defined as any point (x, y) for which T is the object point. It is referred to as the background in order to distinguish it from the rest of the picture. It was once known as global thresholding when the method was solely based on gray-level values; however, when certain local properties were taken into consideration, it was known as local thresholding. It is possible to convert a grayscale image to a binary image using the method developed by Otsu, which is based on thresholds. The optimal boundary between the two classes is determined by assuming that the image histogram has a bimodal distribution. It specifies the initial threshold T as well as the number of groups into which pixels should be divided. The algorithm calculates the histogram and probability for each intensity level by combining the original class probability and mean with the histogram and probability for the intensity level at the time of calculation. To determine the average intensity, the T threshold is calculated and then adjusted in accordance with the results. A specified tolerance between two successive threshold values is observed, and the procedure is repeated until the difference between the two threshold values is less than the specified tolerance. It is the best threshold to use when trying to achieve the best balance of within-class and between-class variance [14].

Image analysis is the process of extracting information from images that can be used to make decisions. Form descriptors are used in a wide range of image processing applications because of their ability to define visually interesting regions in a given image. Consequently, newly developed form descriptors are constantly looking for ways to improve the efficiency of form classification procedures because of this demand [15]. The process of automatically locating and labeling various points within an image is known as automatic image analysis. After performing a pixel-by-pixel scan from left to right and top to bottom, the algorithm moves on to the next step. In order to accurately determine the location of a pixel within an image, each pixel is assigned a label, which is then assigned to the components that have been defined for it. Each class's label corresponds to a

unique entry in a matrix, which is the class-level equivalent of an equivalency class on a higher level of abstraction. Finally, a second image scan is performed to reassign labels to the equivalence class that had previously been assigned to the class itself [6-9]. A label is assigned to each pixel that is a component of a connected component when it is connected. Borders and limits of borders are frequently depicted using a variety of shades of gray and/or colors to represent their boundaries and limits. Objects can be described using the shape parameter or basic geometric parameters after segmentation and labeling of connected components have been applied. These parameters are now well understood. This perimeter can be calculated using the object limit chain code, which combines the length of the chain code with the two-digit values of the diagonal steps to produce a final result that is the perimeter. When the variables N_e and N_o denote the number of uniform and strange string code steps, respectively, and the equation 7 denotes an eight-neighborhood chain code with a perimeter defined by the relationship between n_e and n_o , the result is a code with a perimeter defined by the relationship between n_e and n_o [5].

$$perimeter = n_e + \sqrt[2]{n_o} \quad [1]$$

In order to calculate this distance, multiply the number of sample points by the middle distancing and then take the distance around the boundary line. A critical consideration is the sensitivity of the edge of this form to noise; therefore, it is essential to carefully compare the perimeters of multiple images. Even though the objects' orientations at the image level may be different, the overall orientation of the image remains constant. It makes no difference how an area is rotated or scaled; its roundness and circularity remain constant no matter what [6]. 7 determines whether an object is circular (R), which means that its area is represented by A , which is the number of pixels contained within the object, and its perimeter is represented by P , which is the object's circumference. If an object is circular (R), the fourth step in the function determines whether an object is circular (R). Because of this, a perfectly round region is created, with a value of 1, and everything else has a value in the range between 0 and 1. In this case, the Compactness Factor (CF) is defined as the inverse of this measurement; as a result, this form descriptor contains information about the regularity of an object (equation 8) [6].

$$CR = 4\pi A / P^2 \quad [2]$$

The image spacing of a label object is equal to the spherical equivalent radius of an irregularly

shaped object with a radius of symmetry. In terms of the various forms of extension, it is a very simple and straightforward term. It is necessary to include all of the points that make up a standard measurement in order to put it into effect. When the product of the form's orientation and the moment of inertia equals zero, the last second's moment about the axis occurs. It represents a ratio of the greatest to the second greatest moments, because it represents the time interval between the greatest and second greatest moments, respectively. This object has a monetary value greater than or equal to that of one [12-15].

Methods

This study investigated the detection of cardiac tissue via image processing by utilizing watershed approaches. The two-dimensional cardiac scintigraphs illustrate the SPECT scan results. To preserve the image's quality, JPG files with a high dpi percentage were used. The heart's borders must be separated in order to recognize cardiac tissues. Separating the heart's tissues adequately is crucial. The background image, which is visible in the foreground, shows the uptake of cardiac tissues and other parts of the chest. Extraneous regions of the image were filtered out as noise, allowing for segmentation of the heart tissues and their borders. This enabled segmentation of the cardiac tissues and

their borders. The segmentation procedure is schematically represented in **FIGURE 1**.

Results

MatLab was used to process X-ray pictures of the heart in this investigation. Nuclear cardiology makes use of colored images since they make it easier to distinguish between different tissue types than black and white images do. It is feasible to establish graphic variances while dealing with the CIE $L^*a^*b^*$.

Steps of the segmentation

Step 1: Attaining picture: The image read in MatLab program. (**FIGURE 2**).

Step 2: Changing Image format:

In this step, the image change using makecform and applycform algorithm (**FIGURE 3**).

Step 3: Classify input images into the colour

Step 4: Tag the image elements

Step 5: Segment the H&E image by colour.

The cardiac tissue separate into three images using pixel label, which were shown in **FIGURES 4 and 5**.

Step 6: Segment the result into a distinct Image

Step 7: display all segmentation process

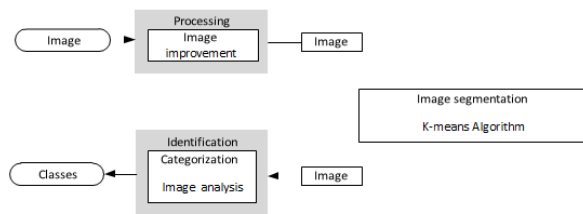


FIGURE 1. The whole Segmentation process.

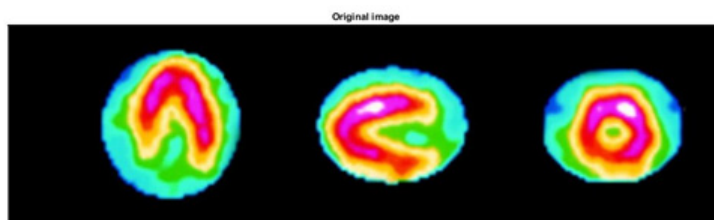


FIGURE 2. The original image.



FIGURE 3. Conversion of colour image.

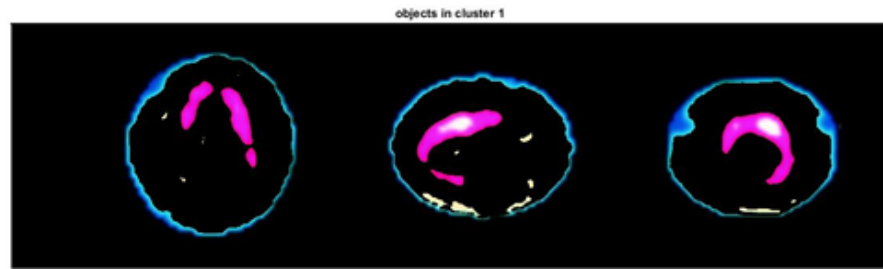


FIGURE 4. Group 1 Cardiac image.

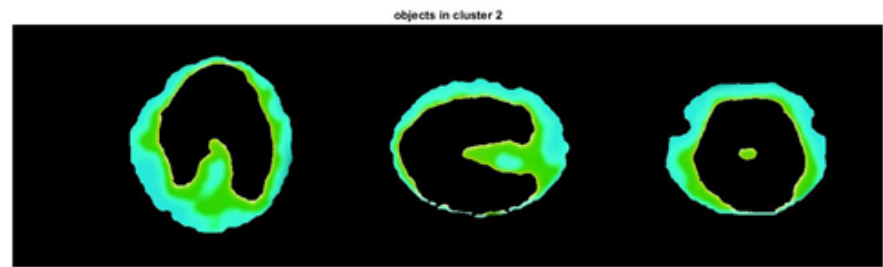


FIGURE 5. Group 2 Cardiac image.

Discussion

Before proceeding with their research, the researchers wanted to ensure that cardiac SPECT data sets were consistently and viably collected in order to generate a template image and execute LV segmentation. After restoring geometric LV perfusion to normal, the researchers employed statistical methods to ascertain the severity of each patient's heart disease condition. K-means segmentation algorithms are used to reveal the heart tissues. This way, heart tissue and disease can be differentiated with extreme precision. The proposed approach, which begins with average image and morphological procedures, noise removal, and border augmentation, is an easy-to-implement segmentation technology. According to TABLE 1 and FIGURE 2-6, the LV structure is partitioned into different segments using K-mean clusters. The Left Ventricle (LV) and Right Ventricle (RV) are depicted in FIGURES 2-6 as being fully distinct from one another. Border identification between the system's numerous separate components, as well as geometrical dimensions and statistical analysis, all contributed to a clear knowledge of their boundaries. The match measure and associated ratio achieved using this method were greater than those reported before by Abdallah [4]. A large cardiac scintogram database has been proved to be accurate and sufficient for usage with this technology. It was demonstrated in this work that utilizing Kmeans algorithms

and clustering approaches, it is possible to discover and define cardiac structures. Future research should incorporate a variety of imaging modalities, which should be factored into the design. Segmentation of the left ventricle is a critical and time-consuming phase in studying the human body with nuclear medicine. The Dice coefficient for this study revealed the accuracy of an automated technique based on K-means clustering (three clusters). We were able to create highly segmented topologies while working with a huge number of data sets, including coronary artery map images. On the other side, the dice coefficient must be modified to approach the maximum feasible value. However, this technique has already proved its capacity to maintain its robust behavior when challenged with noise and low-resolution data. Because the computational technique is more precise, it is significantly more successful when both men and women record SPECT cardiovascular images with dramatically diverse anatomical dimensions. Two significant obstacles confront SPECT image processing: noise and low detail. To address these obstacles, the proposed technique is robust and relies on autonomous computer technology. On the other hand, while the picture logging approach is effective and accurate, it may be improved by increasing the sensitivity value while minimizing the computer's mean error and processing time.

TABLE 1. The statistical results of proposed approach.

	Percentage Match Measure (PM) ($p>0.05$)			Corresponding Ratio (CR) ($p>0.05$)		
	Manual Reading		Automated Reading	Manual Reading		Automated Reading
Average%	Physician 1-5	Physician 6-10	Automated	Physician 1-5	Physician 6-10	Automated
Standard Deviation	81.4%	89.22%	98.91 %	0.06	0.08	-0.07
Minimum	78.4%	81.5%	95.01%	0.01	0.01	0.004
Maximum	85.53%	90.7%	99.1 %	0.10	0.11	1.07

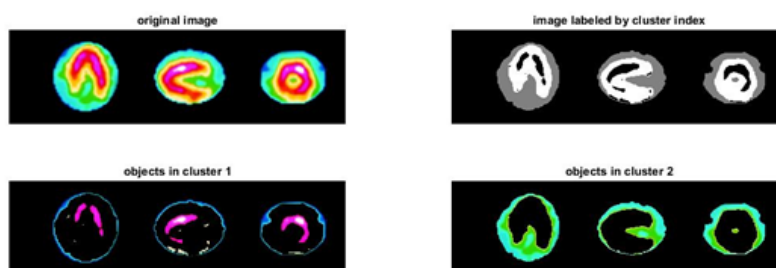


FIGURE 6. Complete segmentation process.

Conclusion

Non-linear smoothing filters have been developed using a variety of techniques. In spite of much research, Fourier is unable to automatically evaluate their merits and applications. Anisotropic and median filtering were used by the researchers to get their findings. Anisotropic and median filtering were used during the testing process.

Acknowledgements

The author is thankful to the Deanship of Scientific Research, at Majmaah University for funding this research..

References

1. Bala A. An improved watershed image segmentation technique using MATLAB. *IJSER*. 3(6), 1-4 (2012).
2. MathWorks Inc. MATLAB User's Guide. The MathWorks Inc., United States of America.42-48 (2021).
3. Petitjean C, Zuluaga MA, Bai W *et al*. Right ventricle segmentation from cardiac MRI: a collation study. *Med Image Anal*. 19(1), 187-202 (2015).
4. Peng P, Lekadir K, Gooya A *et al*. A review of heart chamber segmentation for structural and functional analysis using cardiac magnetic resonance imaging. *Magn Reson Mater Phy*. 29(2), 155-195 (2016).
5. Greenspan H, Van Ginneken B, Summers RM. Guest editorial deep learning in medical imaging: Overview and future promise of an exciting new technique. *IEEE Trans Med Imaging*. 35(3), 1153-1159 (2016).
6. Shen D, Wu G, Suk HI. Deep learning in medical image analysis. *Annu Rev Biomed Eng*. 19, 221-248 (2017).
7. Litjens G, Kooi T, Bejnordi BE *et al*. A survey on deep learning in medical image analysis. *Med Image Anal*. 42, 60-88 (2017).
8. Gandhi S, Mosleh W, Shen J, Chow CM. Automation, machine learning, and artificial intelligence in echocardiography: A brave new world. *Echocardiography*. 35(9), 1402-1418 (2018).
9. Mazurowski MA, Buda M, Saha A, Bashir MR. Deep learning in radiology: An overview of the concepts and a survey of the state of the art with focus on MRI. *J Magn Reson Imaging*. 49(4), 939-954 (2019).
10. Tobon-Gomez C, Geers AJ, Peters J *et al*. Benchmark for algorithms segmenting the left atrium from 3D CT and MRI datasets. *IEEE Trans Med Imaging*. 34(7), 1460-1473 (2015).
11. Bernard O, Lalande A, Zotti C *et al*. Deep learning techniques for automatic MRI cardiac multi-structures segmentation and diagnosis: Is the problem solved? *IEEE Trans Med Imaging*. 37(11), 2514-2525 (2018).
12. Kirişli HA, Schaap M, Metz CT *et al*. Standardized evaluation framework for evaluating coronary artery stenosis detection, stenosis quantification and lumen segmentation algorithms in computed tomography angiography. *Med Image Anal*. 17(8), 859-876 (2013).
13. Bernard O, Bosch JG, Heyde B *et al*. Standardized evaluation system for left ventricular segmentation algorithms in 3D echocardiography. *IEEE Trans Med Imaging*. 35(4), 967-977 (2015).
14. Suinesiaputra A, Cowan BR, Al-Agamy AO *et al*. A collaborative resource to build consensus for automated left ventricular segmentation of cardiac MR images. *Med Image Anal*. 18(1), 50-62 (2014).
15. Karim R, Bhagirath P, Claus P *et al*. Evaluation of state-of-the-art segmentation algorithms for left ventricle infarct from late Gadolinium enhancement MR images. *Med Image Anal*. 30, 95-107 (2016).